



Utilizing Green Chemistry In The Synthesis Of Modified Chitosan Biosorbents: Application In La(III) Ion Recovery From The Monazite Leach Liquor

Waleed M. Semida^a, Ali M. Hassan^b, Tarek F. Mohammaden^a, Sameh H. Negm^a, Mahmoud O. Abd El-Magied^{a,*}

^a Nuclear Materials Authority, P.O. Box 530, El Maadi, Cairo, Egypt

^b Chemistry Department, Faculty of Science, Al-Azhar University, Cairo, Egypt



Abstract

The current study's goal is to use a green synthesis approach in developing some biosorbents for lanthanum (La(III)) recovery from its aquatic media. Chitin (SW-Chitin) was extracted from industrial waste (shrimp waste, SW) by demineralization followed by deproteination reactions. The obtained chitin (SW-Chitin) product was converted to chitosan (SWC) by a deacetylation reaction. The purified chitosan product (PSWC) was modified with epichlorohydrin (ep) in two reaction steps to produce a chitosan-epichlorohydrin polymer (PSWC/ep-Cl). The former product (chitosan-epichlorohydrin polymer, PSWC/ep-Cl) was modified with N,N'-bis(2-aminoethyl)ethane-1,2-diamine, and chloroacetic acid to produce a poly nitrogen biosorbent (PSWC/ep/T-amine) and poly oxygen/nitrogen biosorbent (SWCh/ep/T-amine/PCOOH), respectively. The complexing functionalities of the chitosan backbone have been improved by these moieties (multidentate nitrogen and oxygen donor moieties) to improve the loading capacity, selectivity, and kinetics. The SEM/EDX analysis show that PSWC/EP/T-amine, and PSWC/EP/T-amine/P-COOH mainly composed of nitrogen, and oxygen, hydrogen and carbon. The TGA analysis of PSWC/EP/T-amine, and PSWC/EP/T-amine/P-COOH revealed many periods of mass losses. Also, the dTG (%/min) of PSWC/EP/T-amine and PSWC/EP/T-amine/P-COOH biosorbents contain multiple endothermic peaks. All endothermic peaks in the dTG curves are related to thermal decomposition of PSWC/EP/T-amine and PSWC/EP/T-amine/P-COOH adsorbents. The affinity of SWCh/ep/T-amine and SWCh/ep/T-amine/PCOOH for lanthanum (III) ions was investigated using batch technique. The maximum uptake of lanthanum ions by SWCh/ep/T-amine and SWCh/ep/T-amine/PCOOH was achieved at pH 7 and 328K were 98.2 and 129.6 mg/g, respectively. The results refers to a chemisorption reaction of lanthanum ions with the PSWC/EP/T-amine and PSWC/EP/T-amine/P-COOH adsorbents controlled intraparticle diffusion mechanism. The isotherm and thermodynamic evaluation refers to spontaneous, endothermic, monolayer adsorption of lanthanum ions on the PSWC/EP/T-amine and PSWC/EP/T-amine/P-COOH adsorbents.

Keywords: La(III); Green Synthesis; Biosorbent; Adsorption; Monazite.

1. Introduction

Lanthanum is a rare earth element commonly found in conjunction with cerium and other rare earth elements in rare-earth minerals such as cerite,

monazite, allanite, and bastnäsite [1-3]. Lanthanum is the 28th most abundant element in the Earth's crust, over three times more abundant than lead. Monazite is a rare phosphate mineral with the general formula of (Ce, La, Nd, Th)(PO₄,SiO₄). In the structure of the monazite mineral, cerium (Ce), lanthanum (La), neodymium (Nd), and thorium (Th) may all replace one another, and silica (Si) can also replace

*Corresponding author e-mail: mahmoud_nma@yahoo.com (Abd El-Magied).

Received date 2023-04-03; revised date 2023-05-20; accepted date 2023-05-22

DOI: 10.21608/EJCHEM.2023.203780.7815

©2023 National Information and Documentation Center (NIDOC)

phosphate (PO_4) [4,5]. Also, secondary sources of lanthanum (In-use stocks such as catalysts and magnets in automobiles and wind turbine) have attracted more attention due to their dramatically increasing number of applications and significant growth in global consumption [3-6]. Naturally occurring lanthanum contains two isotopes, ^{139}La (99.910% of natural lanthanum) and ^{138}La (0.088%). In chemical reactions, lanthanum loses its valence electrons to produce the +3 oxidation state [2, 5]. Lanthanum possesses the lanthanides' biggest atomic radius. As a result, it is the most reactive, it may form binary compounds with nonmetals such as carbon, nitrogen, phosphorus, sulphur, and selenium. Lanthanum has restricted coordination chemistry due to the large ionic radius and high electropositivity of its ions. The most common donor atom in lanthanum complexes is oxygen, (usually ionic and having high coordination numbers, 6 to 12) [4-6]. Lanthanum is a key constituent in the development of the high-tech industry, including high-tech devices, batteries, alloys, catalysts, medical, semiconductors, and ceramics industries [2, 7]. As these industry sectors are growing, the global consumption of lanthanum is going to increase dramatically while the supply is diminishing. Also, effluents from these applications are often associated with high concentrations of lanthanum. Therefore, there is scope for extracting lanthanum from its sources as well as from its application effluents. The separation of lanthanum from its sources is a difficult procedure because of its low concentration and the usually complex nature of the host sources. Moreover, REEs have similar physiochemical properties, which makes the individual separation of lanthanum them very challenging. Solid phase extraction (or solid-liquid extraction) is an excellent technique for the separation and preconcentration of different adsorbates (ions or molecules) from various geological and water systems. Solid phase extraction is dependent on the transfer of soluble components from the aqueous phase to the active sites of the adsorbent which is controlled by the type and sensitivity of active groups, their pH sensitivity, the degree of their ionization, and the backbone structure. The metal, after sorption on the solid phase, is desorbed with a suitable eluate and thus recovered. Solid phase extraction affords a broader range of application than solvent extraction due to the large choice of solid adsorbents. Among the different separation and purification techniques, the separation and extraction of lanthanum using biosorbents is heavily relied upon due to several advantages such as efficiency, simplicity, selectivity, eco-friendliness, and economy, especially for the effluent treatment and recovery of lanthanum. Recently, natural biosorbents, such as lignin, chitosan, cellulose, and

alginate-based adsorbents, have been proposed as efficient materials for recovering rare earth elements and other metals from their sources [8-11]. Almost half or more of the mass of shrimp is wasted during processing in the shrimp industry. This waste product contains $\text{Ca}_3(\text{PO}_4)_2$, CaCO_3 , protein and chitin [11,12]. So, by removing $\text{Ca}_3(\text{PO}_4)_2$, CaCO_3 , and protein content, chitin is obtained [11,12]. Chitin is transform into chitosan by de-acetylation reaction (partial or complete removing of acetyl groups from the chitin molecule). Chitosan has enhanced characteristics and attracted growing economic attention than chitin because of its biocompatibility, solubility, and availability of modification methods with various ligands [12]. Different chitosan-based biosorbents were synthesized and used in lanthanum (III) ion adsorption. Adsorption of La(III) from aqueous solutions has been investigated in batch and continuous modes using chitosan-poly(vinyl alcohol)-3-mercaptopropyltrimethoxysilane adsorbent [14]. The optimum pH for La(III) adsorption was found to be pH 5. The synthesized polyethylene imine chitosan adsorbents showed selective adsorption affinities for La(III) from Al(III) in the pH range of 1-3.5 [15]. Modified mesoporous silica/chitosan adsorbents were synthesized for La(III), Sc(III), and Y(III) separation from single and multi-component acidic solutions (pH 3) [16]. Acrylo-thiourea-chitosan adsorbents showed adsorption behaviors for lanthanum (III) from aqueous chloride medium with a maximum uptake capacity of 2.1 mmol/g [17]. A manganese dioxide-formaldehyde-chitosan nanocomposite has been synthesized to remove lanthanum ions from water (pH 6) with a capacity value of 1050 $\mu\text{mol/g}$ at pH 6 [18]. The current study's goal is to develop some biosorbents for lanthanum (La(III)) biosorption and recovery from its aquatic media. The biosorbents were modified with different multidentate nitrogen and oxygen donor coordinating ligands. The affinity of biosorbents for lanthanum (III) ions from synthetic and leach liquor was investigated and discussed.

2. Experimental

2.1. Chemicals

The used shrimp waste (from a local fishing market) was used as the base material for adsorbent synthesis. Nitric acid, hydrochloric acid, acetic acids, sodium hydroxide, ethanol, N,N-dimethylformamide, epichlorohydrin (EP), N,N'-bis(2-aminoethyl)ethane-1,2-diamine (T-amine), and lanthanum nitrate hexahydrate were Sigma-Aldrich chemicals. Water (double distilled) was used to make all of the solutions that were employed in this investigation. A

0.01 M solution of NaOH and HCl was used to solution accuracy pH adjustment. The initial and final concentration (C_i and C_e) of lanthanum (III) ions was determined using Arsenazo III (Arz III) method, with absorbance measured spectrophotometrically at $\lambda = 650$ nm [19].

2.2. Synthesis of SWCh/ep/T-amine and SWCh/ep/T-amine/PCOOH Biosorbents

100 g of SW was stirred in a 1000 mL 2M HCl (solid: liquid = 1:10) for 24 h, after which the suspension was irradiated in a microwave. The solid residue was washed with distilled water, and dried at 80°C. The demineralized product obtained (DMSW) was added to 1000 ml NaOH (10 %), (solid: liquid = 1:10) and stirred overnight. The suspension of DMSW was irradiated in a microwave. The residue was filtered (SW-Chitin) and washed with water, and dried at 80°C to give chitin product (SW-Chitin). The chitin product (SW-Chitin) was added and stirred in 1000 ml NaOH (60 %), (solid: liquid = 1: 15) overnight. The suspended SW-Chitin was irradiated in a microwave. The solid residue was washed, and dried at 80°C to give chitosan product (SWC). The chitosan product (SWC) was dissolved in acetic acid (2%), stirring at room temperature, and 24 h until the complete dissolution or clear solution was obtained. In 1 L of NaOH (2M) containing 10% ethyl alcohol, the SWC was subsequently precipitated. Filtered chitosan gel was thoroughly cleaned to a pH of about 7 to obtain purified chitosan (PSWC). The purified chitosan (PSWC) was stirred in NaOH solution (pH=10, 298K, 120 min). 2-Propanol was added to the PSWC solution and then the PSWC solution was stirred for 30 min. Under stirring, epichlorohydrin (EP, 35 mL) was added dropwise (over 35 min) to the PSWC/2-propanol solution. The PSWC/2-propanol/EP solution was irradiated in the microwave. The residue (chitosan-epichlorohydrin polymer, PSWC/EP) was filtered from the PSWC/2-propanol/EP solution and then the PSWC/EP was washed with H₂O, dil NaOH, dil HCl, and H₂O, respectively, and dried at 80°C. The product obtained (PSWC/EP) was stirred in isopropanol alcohol (75 mL, 298K, 15 min), and then epichlorohydrin and acetone solution were added to the PSWC/EP/isopropanol alcohol mixture. After 60 min of stirring, the PSWC/ep/isopropanol alcohol mixture was irradiated in microwave, and the residue (chitosan-epichlorohydrin-Cl polymer, PSWC/EP-Cl) was filtered off. Wash the PSWC/ep-Cl with H₂O, and then dried it at 353 K. The chitosan-epichlorohydrin-Cl product, PSWC/EP-Cl, was added to ethanol solution (100 ml, 1:1) and then the PSWC/EP-Cl /ethanol solution was stirred for 35 min. Under stirring, N,N'-bis(2-aminoethyl)ethane-

1,2-diamine (T-amine, 75 mL) was added dropwise (over 40 min) to the PSWC/ep-Cl /ethanol solution. The PSWC/EP-Cl /ethanol/T-amine solution was irradiated in the microwave. The residue was filtered off and washed with H₂O, and dried (353 K) to give amine chitosan polymer (PSWC/EP/T-amine). The PSWC/ep/T-amine product was added to isopropyl alcohol (100 mL) and then the PSWC/ep/T-amine/isopropyl solution was stirred for 120 min. Under stirring, NaOH was added dropwise (over 35 min) to the PSWC/ep/T-amine/isopropyl solution followed by the drop wise addition of chloro-acetic/isopropyl alcohol solution (1:1). The PSWC/ep/T-amine/isopropyl/chloro-acetic solution was irradiated in the microwave for 10 minutes (five times). The solid residue (PSWC/EP/T-amine/P-COOH) was washed, and dried, 353 K.

2.3. Biosorption of Lanthanum (III) Ions on the PSWC/EP/T-amine and PSWC/EP/T-amine/P-COOH Biosorbents

Adsorption experiments of La(III) under controlled pH were achieved by adding 25.0 mg of PSWC/ep, PSWC/EP/T-amine and PSWC/EP/T-amine/P-COOH adsorbents in a series of flasks. In each flask, 50.0 mL solution of 200.0 mg/L of La(III) (pH 1 - 7) were added. The suspended PSWC/ep, PSWC/ep/T-amine and PSWC/ep/T-amine/P-COOH adsorbents into La(III) solution were stirred (200 rpm) for 4.0 h at room temperature. After equilibration, PSWC/EP, PSWC/EP/T-amine and PSWC/EP/T-amine/P-COOH loaded with La(III) were removed from the adsorption medium, and the final (or remaining) La(III) concentration was determined spectrophotometrically. The adsorption capacity of PSWC/EP, PSWC/EP/T-amine and PSWC/EP/T-amine/P-COOH (mg/g) and their efficiency (%) were computed from the equations 1 and 2, respectively [20].

$$q_e \text{ (mg/g)} = \frac{C_i - C_e}{\text{Sorbent weight}} \times V \quad (1)$$

$$q_{ef} \text{ (%) } = 100 \times \frac{C_i - C_e}{\text{Adsorbent weight}} \quad (2)$$

Where q_e (mg/g) and q_{ef} (%) are the adsorption capacities and efficiency at equilibrium, respectively. C_i , C_e , and V are the initial and final concentrations (mg/L) of La(III), and the volume (L) of the solution, respectively. The amount of La(III) adsorbed at different time periods was obtained by stirring 25.0g of PSWC/EP/T-amine and PSWC/EP/T-amine/P-COOH in a 50.0 ml 200 mg/L of La(III) solution (pH 7). The contents of the adsorption system were shaken (200 rpm) at 298 K for the required time period. The final concentration of lanthanum(III) ion was measured after equilibration. Adsorption isotherms of La(III) on PSWC/EP/T-amine and PSWC/EP/T-amine/P-COOH were obtained by stirring 25.0 mg of PSWC/EP/T-amine and

PSWC/EP/T-amine/P-COOH in La(III) solution (50 mL at pH 7) with different initial concentrations of La(III). The contents of the flasks were equilibrated on the shaker at 200 rpm while keeping the temperature at 298, 308, 318 and 328K for 2 h. After equilibration, the residual concentrations of La(III) were determined. The solid/liquid ratio was tested using different doses of the PSWC/EP/T-amine and PSWC/EP/T-amine/P-COOH into the adsorption La(III) solution, while keeping other optimize condition constant.

3. Results and Discussion

3.1. Synthesis and Characterization of the PSWC/EP/T-amine and PSWC/EP/T-amine/P-COOH Adsorbents

A shrimp chitosan product was obtained from shrimp waste in three main steps using a green synthesis approach. The various characteristics of SW, SW-chitin, PSWC, PSWC/EP, PSWC/EP/T-amine and PSWC/EP/T-amine/P-COOH biosorbents were determined. Chitin recovered from SW had a yield of 21.9%. The moisture content of PSWC/EP, PSWC/EP/T-amine and PSWC/EP/T-amine/P-COOH is 8.96, 9.35, and 8.87, respectively. Figure 1 shows the object's FT-IR spectrum of PSWC, PSWC/EP/T-amine and PSWC/EP/T-amine/P-COOH. The spectrum of PSWC contains bands at wavenumbers of (cm^{-1}) of 3442 (OH and NH vibrations), 3276 (moisture content, OH and NH_2 bonds), 3109 (stretching NH symmetric), 2923 and 2852 (CH and CH_2 groups), 1660 and 1629 (C-N and C=C bonds), 1564, 1419 and 1337 (C-O, C-N, N-H and CH_2 bonds), 1315 (C-N bond), 1257 (NH bond), 1151 (C-OH, C-O and C-O-C bonds of the chitosan ring), 1074, and 1024 (C-C, C-O, O-CH, and C-O-H bonds of chitosan ring). Also, the PSWC spectra contains bands at wavenumbers of (cm^{-1}) 742, 700 and 590 related to vibrational (bending) of C-C and C=C bonds of chitosan (PSWC) [21, 22]. The spectra of PSWC/EP/T-amine contains bands at wavenumbers of (cm^{-1}) 3357.60 (OH and NH), 3284.32 (moisture content, OH and NH_2 bonds), 2892.82 and 2879.32 (CH), (CH_2), 2208.19 and 2050.05 (C-N), 1647 (C=C), 1637.34 and 1560.20 (C-N and NH_2 bond), and at 1456.05 (C-H bending). Also, the spectrum of PSWC/EP/T-amine contains bands at wavenumbers of (cm^{-1}) 1373.13, 1313.34 and 1247.77 (methylene, OH bending and C-N stretching), 1024.06 (aliphatic NH and NH_2), 630.64, 595.43 and 561.21 (C-C, C-N, and C=C) [21, 22]. The spectra of PSWC/EP/T-amine/P-COOH contains bands wavenumbers of (cm^{-1}) 3259 (OH and NH), 2937 (CH_2), 2892 and 2634 (CH_2), 1727 (non-ionized

COOH), 1627 (C=O from COOH), 1413 and 1376 ($\text{CH}_2=\text{CH}_2$), 1222 cm^{-1} (C-O of from COOH), 1058 (C-O of C-OH and C-N vibrations), 898 ($\text{C}=\text{CH}_2$), and 784, 657 and 620 (C=O and C=C) [21,22]. Also, the spectra of PSWC/EP/T-amine/P-COOH contains bands at 578, 559, 464, 443 and 418 (C-O, C-C and C-N).

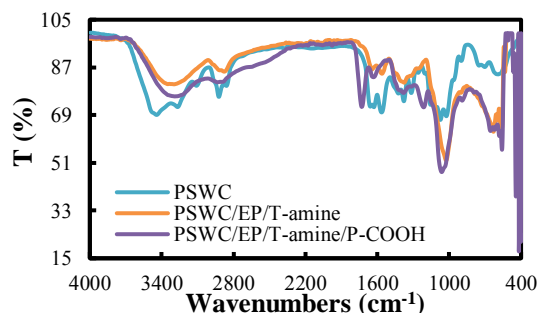


Fig. 1. FTIR spectra of PSWC, PSWC/EP/T-amine and PSWC/EP/T-amine/P-COOH adsorbents

SEM/EDX analysis (from Scanning Electronic Microscope/Energy Dispersive X-ray Spectrometer) was used to analyze the surface characteristics of PSWC, PSWC/EP, PSWC/EP/T-amine, and PSWC/EP/T-amine/P-COOH. The sorption of lanthanum ions cause a change in the surface appearance of the PSWC/EP/T-amine, and PSWC/EP/T-amine/P-COOH surface. The SEM/EDX analysis show that PSWC/EP/T-amine, and PSWC/EP/T-amine/P-COOH mainly composed of nitrogen, and oxygen, hydrogen and carbon. (Fig. 2). SW, PSWC, PSWC/EP/T-amine, and PSWC/EP/T-amine/P-COOH had surface areas of 51.53, 12.71, 43.59, and 23.91 m^2/g , respectively.

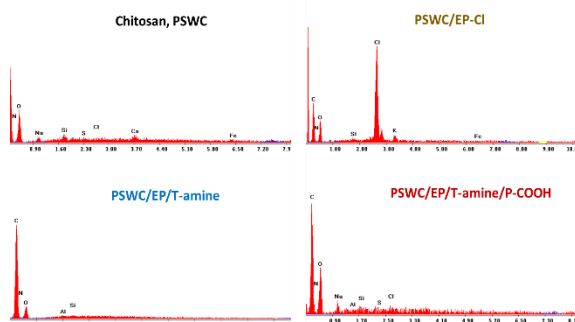


Fig. 2. EDX analysis of PSWC, PSWC/EP-Cl, PSWC/EP/T-amine, and PSWC/EP/T-amine/P-COOH biosorbents

Thermogravimetric analysis (TGA) is one of the crucial thermal analytical methods used to examine the thermal stability of polymers [23, 24]. TGA shows the relationship between weight losses and

temperature. The TGA analysis of PSWC/EP/T-amine, and PSWC/EP/T-amine/P-COOH revealed many periods of mass losses. Also, the dTG (%/min) of PSWC/EP/T-amine and PSWC/EP/T-amine/P-COOH biosorbents contain multiple endothermic peaks. All endothermic peaks in the dTG curves are related to thermal decomposition of PSWC/EP/T-amine and PSWC/EP/T-amine/P-COOH adsorbents.

3.2. Effect of Solution pH

The acidity of the solution is one of the most significant factors affecting lanthanum adsorption on PSWC/EP, PSWC/EP/T-amine, and PSWC/EP/T-amine/P-COOH adsorbents. The pH controls the surface charge of the PSWC/EP, PSWC/EP/T-amine, and PSWC/EP/T-amine/P-COOH and influences the lanthanum speciation. The affinity of PSWC/EP, PSWC/EP/T-amine, and PSWC/EP/T-amine/P-COOH for lanthanum (III) ions was investigated using batch technique. Fig. 3 shows the effect of medium pH on the lanthanum adsorption by PSWC/EP, PSWC/EP/T-amine, and PSWC/EP/T-amine/P-COOH adsorbents. The uptake of lanthanum(III) ions by PSWC/EP, PSWC/EP/T-amine, and PSWC/EP/T-amine/P-COOH was very low at pH < 1, and it increased with the increase of pH till reached maximum value at the limit at pH 7.0, for both adsorbents. The maximum uptake of lanthanum ions by PSWC/EP, PSWC/EP/T-amine, and PSWC/EP/T-amine/P-COOH achieved at pH 7.0 were 57.4, 73.8 and 101.4 mg/g, respectively. At very low pH, lanthanum species cannot bind the adsorbent surface because of electrostatic repulsion with the protonated adsorbent surface. This behavior resulted in a low lanthanum uptake at low pH values. Also, the H⁺ ion from the adsorption medium) compete with lanthanum species for the adsorbent binding groups. Additionally, the larger ionic radius of lanthanum species makes their adsorption difficult. With increasing pH; the ability of the biosorbents to protonate weakens (amino groups deprotonate), carboxylate groups mostly occur as COO⁻ anions (ionized) and consequently increasing La(III)/biosorbents interaction (increasing adsorption) [25].

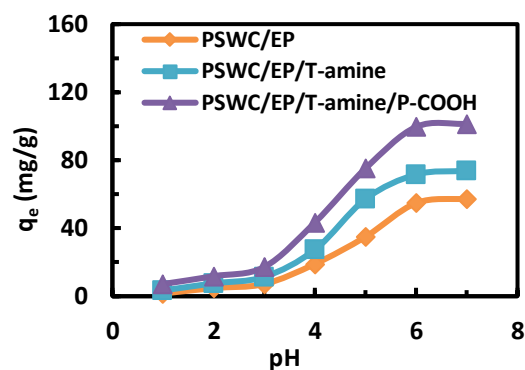


Fig. 3. Effect of solution pH on uptake of lanthanum ions PSWC/EP, PSWC/EP/T-amine, and PSWC/EP/T-amine/P-COOH

In addition, the distribution of lanthanum ion species may play an important role in the adsorption process. At pH 1-3 and 3-8, the main species of La(III) are La₅(OH)₉⁶⁺ and La³⁺, respectively. La³⁺ species are more easily adsorbed on the sorbent than La₅(OH)₉⁶⁺. As a result, increasing pH improves La(III) uptake capacity by increasing the availability of La³⁺ (relatively smaller ionic radius) rather than La₅(OH)₉⁶⁺ (relatively larger ionic radius). This behavior results in enhanced separation of lanthanum at higher pH values. So, the pH was optimized at 7, which was used in the following experiments.

3.3. Effect of Contact Time

The contact time is another performance governing factor in adsorption process, as contact time can influence the economic efficiency and kinetics of the adsorption process. Therefore, the sorption experiments were carried out by stirring the PSWC/EP/T-amine and PSWC/EP/T-amine/P-COOH biosorbents into the lanthanum solutions (200 mg/L) for the required time period. The remaining La(III) concentrations was analyzed after PSWC/EP/T-amine and PSWC/EP/T-amine/P-COOH adsorbents filtration. Figure 4 depicts the amount of La (III) ions adsorbed into PSWC/EP/T-amine and PSWC/EP/T-amine/P-COOH vs time.

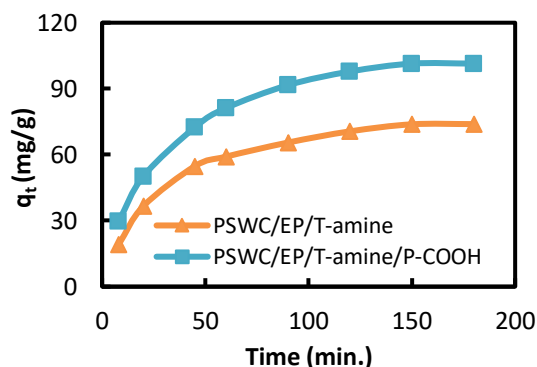


Fig. 4. Effect of time on lanthanum adsorption by PSWC/EP/T-amine and PSWC/EP/T-amine/P-COOH.

It is obvious that, the adsorbed lanthanum(III) ions into PSWC/EP/T-amine and PSWC/EP/T-amine/P-COOH rose monotonically till it arrive the plateau at 150 minutes. About 25.88 and 29.23% of the total adsorbed lanthanum ions were adsorbed in less than 10 minutes by PSWC/EP/T-amine and PSWC/EP/T-amine/P-COOH, respectively. This Initial fast kinetic rate is related to the higher initially unoccupied active sites of PSWC/EP/T-amine and PSWC/EP/T-amine/P-COOH and also due to greater ratio of lanthanum ions to the active sites of PSWC/EP/T-amine and PSWC/EP/T-amine/P-COOH. With time, the unoccupied active sites of PSWC/EP/T-amine and PSWC/EP/T-amine/P-COOH and the ratio of lanthanum ions to the active sites of PSWC/EP/T-amine and PSWC/EP/T-amine/P-COOH decreased, which lowers the amount of lanthanum adsorption. About 74.25 and 71.51% of the total adsorbed lanthanum ions (73.8 and 101.4 mg/g) were adsorbed in less than 45 minutes by PSWC/EP/T-amine and PSWC/EP/T-amine/P-COOH, respectively.

3.4. Adsorption Kinetics

The design the adsorbent depend heavily on the rates of adsorption since sorption process is a time-dependent process. Kinetic models are used to assess the experimental data in order to predict the mechanism of the adsorption process. The kinetic studies shed light on the non-equilibrium steps of the sorption mechanism and the rate at which the process takes place. The kinetic evaluation was studied to explain the rate at which La(III) is adsorbing onto PSWC/EP/T-amine and PSWC/EP/T-amine/P-COOH. Kinetic evaluation has been described by a number of adsorption kinetic models. The rate and order of the adsorption reactions are often explained by two widely used kinetic models, pseudo-first-order (Eq. 3) and pseudo-second-order (Eq. 4). Pseudo-first order reactions are those that are not first-order but have the appearance of being first-order because one or more of the reactants are present

at higher concentrations (However, because the total variation in its concentration is so little, it is regarded as constant) than the others. Consequently, the concentration of the adsorbate is used to indicate the rate of the adsorption process. The pseudo-first-order kinetic model was used to analyze the current adsorption data using equation (6) [26].

$$\log (q_e - q_t) = \log Q_1 - \frac{1}{2.303} K_1 t \quad (3)$$

where q_t (mg/g), Q_1 (mg/g), and k_1 (min^{-1}) represents adsorption capacity at time (t), pseudo first adsorption capacity, and the pseudo first rate constant of the adsorption process, respectively. For pseudo-first-order order kinetic model, plotting the values of $\log (q_e - q_t)$ versus corresponding contact time (t) should give a straight line with slope and intercept equals the values of $(-k_1/2.303)$ and $(\log Q_1)$, respectively. According to pseudo-first-order order kinetic plots (Fig. S1, Supplementary file), plotting the values of $\log (q_e - q_t)$ versus corresponding contact time (t) gave a straight line with slope and intercept equals the -0.0105 and 1.7958 for lanthanum adsorption PSWC/EP/T-amine, and -0.0113 and 1.9583 for lanthanum adsorption by PSWC/EP/T-amine/P-COOH, respectively. The values of Q_1 (mg/g), and k_1 (min^{-1}) were calculated from these values and were represented in Table 1. The inconsistency of the values of q_e (73.8 and 101.4 mg/g) with the value of Q_1 (62.49 and 90.85 mg/g) for lanthanum adsorption on both PSWC/EP/T-amine and PSWC/EP/T-amine/P-COOH, refers to unsuitability of the pseudo-first-order order kinetic model to describe the studied adsorption process. Also, the small value of R^2 (< 0.995) of this kinetic models confirms this hypothesis. The pseudo-second-order kinetic equation (Eq. 4) is used to analyze the mechanism of lanthanum adsorption by PSWC/EP/T-amine and PSWC/EP/T-amine/P-COOH. When the rate-determining step is seen as a chemisorption of the adsorbent on the adsorbate (chemisorption processes), the pseudo-second-order kinetic model offers the best correlation adsorption mechanism of the experimental adsorption data. The pseudo-second-order kinetic model predicts behavior across the whole adsorption range and is dependent on the presumption that chemical sorption or chemisorption is the rate-limiting phase. Adsorption rate in this situation is determined by adsorption capacity rather than adsorbate concentration. The theoretical equilibrium adsorption capacity can be predicted from the model, which is a significant benefit of this model over pseudo-first-order kinetic model. Pseudo-second-order kinetic equation (Eq. 4) was used to analyze the mechanism of sorption and possible rate-controlling step of the current adsorption data [27].

$$\frac{t}{q_t} = \frac{t}{q_e} + \frac{1}{Q_2^2 k_2} \quad (4)$$

Where Q_2 (mg/g), and k_2 (g/mg.min) represents pseudo second adsorption capacity, and the pseudo second rate constant of the adsorption process, respectively. For pseudo-second-order kinetic model, plotting the values of (t/q_t) versus corresponding contact time (t) should give a straight line with slope and intercept equals the values of $(1/Q_2)$ and $(1/k_2.Q_2^2)$, respectively. According to pseudo-second-order kinetic plots (Fig. S2, Supplementary file), plotting the values of (t/q_t) versus corresponding contact time (t) gave a straight line with slope and intercept equals the 0.0115 and 0.322 for lanthanum adsorption by PSWC/EP/T-amine, and 0.0084 and 0.2257 for lanthanum adsorption by PSWC/EP/T-amine/P-COOH, respectively. The values of Q_2 (mg/g), and k_2 (min^{-1}) were calculated from these values and were represented in Table 1. The consistency of the values of q_e (73.8 and 101.4 mg/g) with the value of Q_2 (86.96 and 119.05 mg/g) refers to suitability of the pseudo-second-order kinetic model to describe the studied adsorption process. Also, the higher value of R^2 (≥ 0.9991) of this kinetic models confirms this hypothesis, so, La(III) adsorption on PSWC/EP/T-amine and PSWC/EP/T-amine/P-COOH is suggested to be chemisorption process. Intraparticle diffusion and Elovich models were employed to analyze the role of intraparticle diffusion and adsorbent/adsorbate interaction on lanthanum adsorption. The adsorption/time data for lanthanum adsorption on PSWC/EP/T-amine and PSWC/EP/T-amine/P-COOH were investigated using the intraparticle diffusion kinetic model (Eq. 5) to evaluate the impact of intraparticle diffusion in the lanthanum adsorption process [28].

$$q_t = C + k_{IPDM}t^{0.5} \quad (5)$$

Where q_t (mmol/g) is the lanthanum adsorption capacity at time t, k_{IPDM} (mmol/g.min^{0.5}) is the intraparticle diffusion rate constant, and C is the intraparticle diffusion constant. The plots of q_t vs $t^{0.5}$ should represent straight lines if the overall adsorption rate is intraparticle diffusion-controlled step. The values of constant (C) reveal details about the boundary layer's thickness. The bigger influence of the boundary layer is implied by a larger constant (C). The graphs of q_t vs. $t^{0.5}$ for the lanthanum adsorption on PSWC/EP/T-amine and PSWC/EP/T-amine/P-COOH are depicted in Fig. S3, Supplementary file. The resultant plots show lines that are almost perpendicular to the origin (C = 0.0763 and 0.1144 for the lanthanum adsorption on PSWC/EP/T-amine and PSWC/EP/T-amine/P-COOH, respectively) and allude to intraparticle diffusion as the rate-determining step. The Elovich equation (Eq. 6) is a commonly used in describing the kinetics of chemical adsorbate-determining [29]:

$$q_t = \frac{1}{b} \ln(1 + abt) = \frac{1}{b} \ln(ab) + \frac{1}{b} \ln(t) \quad (6)$$

Where the constants (a) and (b) are constants related to the initial biosorption rate (mg/(g.min)) and

desorption rate (g/mg), respectively. Fig. S4 (Supplementary file) shows the Elovich plots of lanthanum adsorption on the PSWC/EP/T-amine and PSWC/EP/T-amine/P-COOH adsorbents. The slope and intercept of the Elovich plots were used to derive the corresponding kinetic parameters for the model. (Table 1). The Elovich equation fit the adsorption time-dependent data better, with $R^2 \geq 0.9958$. The outcome of the Elovich model indicates chemisorption of lanthanum into the used adsorbents (through exchange or transfer of electrons between lanthanum and adsorbents).

3.5. Effect of Adsorbate Concentration

The initial concentration was related to the driving force of the adsorbate molecules to the active site of the adsorbent. Thus, this parameter had an impact on how adsorbent and adsorbate interacted in the solution. Various concentrations of lanthanum(III) ions (25–400 mg/L) were used to examine the impact of initial metal ion concentration on the adsorption performance. A 50 mL solution of La(III) (at pH 7, and at different initial concentration) were added to the PSWC/EP/T-amine and PSWC/EP/T-amine/P-COOH biosorbents. The samples were shake at 27 °C for 150 minutes. The samples were eventually collected, filtered, and analyzed using spectrophotometry. Fig. 5 shows the effect of adsorbate concentration on lanthanum adsorption by PSWC/EP/T-amine and PSWC/EP/T-amine/P-COOH adsorbents. According to the findings, the lanthanum adsorption capacity on PSWC/EP/T-amine and PSWC/EP/T-amine/P-COOH increased monotonically with increase adsorbate concentration till it arrive the plateau at adsorbate concentration of 300 mg/L. This conduct might be a consequence of increase availability of active sites on PSWC/EP/T-amine and PSWC/EP/T-amine/P-COOH per lanthanum ion in the adsorption medium.

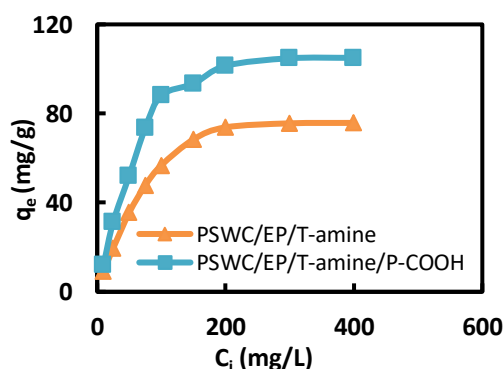


Fig. 5. The effect of adsorbate concentration on lanthanum adsorption by PSWC/EP/T-amine and PSWC/EP/T-amine/P-COOH

Table 1
The kinetic parameters obtained from kinetic modelling of lanthanum adsorption on PSWC/EP/T-amine and PSWC/EP/T-amine/P-COOH adsorbents

Model	Parameters	Value	
		PSWC/EP/T-amine	PSWC/EP/T-amine/P-COOH
Experimental adsorption capacity	qt	73.8	101.4
Pseudo first order	Q1	62.49	90.84
	k1st	1.7958	1.9583
	R2	0.9915	0.9948
Pseudo second order	Q2	86.96	119.05
	K2	0.0004	0.0003
	R2	0.9996	0.9991
Intraparticle diffusion rate model	kIPDM	0.0404	0.0546
	C	0.0763	0.1144
	R2	0.9323	0.9512
Elovich	a	6.78	9.93
	b	0.0530	0.0395
	R2	0.9958	0.9974

3.6. Effect of Adsorption Temperature

The impact of temperature on lanthanum adsorption by PSWC/EP/T-amine and PSWC/EP/T-amine/P-COOH was studied at temperatures range of 298-328 K. Figure 6 shows the values of q_e of lanthanum adsorption by PSWC/EP/T-amine and PSWC/EP/T-amine/P-COOH vs temperature (298-328K). The progressive increase in lanthanum adsorbed quantities together with the rise in ambient temperature indicates that the current process was endothermic. Also, this conduct relates to the chemisorption of lanthanum adsorption on PSWC/EP/T-amine and PSWC/EP/T-amine/P-COOH adsorbents. If the adsorption process is chemisorption, higher adsorption would be obtained at a higher temperature since the rate of chemical reaction rises with rising temperature. Also, changes in temperature might chemically affect the adsorbent, its adsorption sites, and its activity. So, the endothermic and chemical nature character of the sorption process was indicated by the higher adsorption capacities at higher temperatures [30].

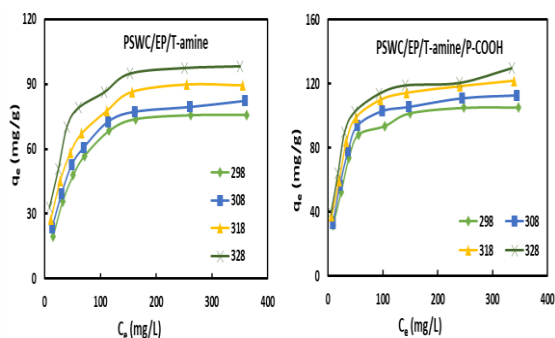


Fig. 6. The temperature effect on lanthanum adsorption by PSWC/EP/T-amine and PSWC/EP/T-amine/P-COOH.

3.7. Adsorption Isotherm Evaluation

An adsorption isotherm is a curve that expresses the change in total quantity of adsorbate that is adsorbed on the adsorbent with its concentration at constant temperature. Adsorption isotherm models may explain the interaction processes between the adsorbent and the adsorbate at constant temperature by taking into account the equilibrium data and the adsorption characteristics of both the adsorbent and the adsorbate. Therefore, one of the most important ways to predict adsorption mechanisms of distinct adsorption systems is to understand the adsorption isotherms of the equilibrium data. The equilibrium data of lanthanum adsorption by PSWC/EP/T-amine and PSWC/EP/T-amine/P-COOH adsorbents were modeled according to various adsorption isotherm models (using their linear regression analysis) to choose the optimum adsorption isotherm model for adsorption data optimization. The Langmuir model describes monolayer adsorption systems with a finite number of identical potential energy adsorption sites on the adsorbent. The Langmuir adsorption model is assumed that there is no lateral contact between adsorbate species and that the reactive groups are uniformly distributed throughout the surface of the adsorbent particle. The equilibrium data of lanthanum adsorption by PSWC/EP/T-amine and PSWC/EP/T-amine/P-COOH adsorbents were modeled according to Langmuir isotherm, Eq. 7 [31].

$$\frac{C_e}{q_e} = \frac{1}{Q_L K_L} + \frac{C_e}{Q_L} \quad (7)$$

where C_e and q_e are equilibrium lanthanum concentration (mg/L) and adsorption capacity (mg/g), respectively. Q_L and K_L are saturation capacity, theoretical amount, (mg/g) and Langmuir binding constant (L/mg), respectively. According to Langmuir isotherm equation, plotting the values of (C_e/q_e) against the values of (C_e) of lanthanum adsorption by PSWC/EP/T-amine and PSWC/EP/T-amine/P-COOH adsorbents gives straight lines with

slope and intercept equals the value of $(1/Q_L)$ and $(1/Q_L K_L)$. The Langmuir model's linear regression is shown in Figure 7.

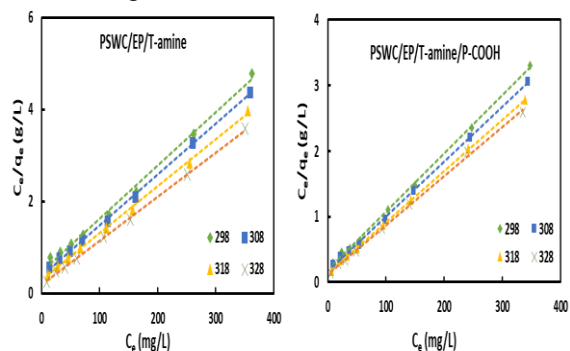


Fig. 7. Langmuir isotherm of lanthanum adsorption by PSWC/EP/T-amine and PSWC/EP/T-amine/P-COOH.

The values of Langmuir parameters (Q_L and K_L) at different temperatures were figured using the slopes and intercepts of the obtained straight lines, and were tabulated. The results (Fig. 7) show that the values of both Q_L and K_L are increased with increase temperatures. The increase in K_L with temperature refers to increase interaction between binding between lanthanum ions and PSWC/EP/T-amine or PSWC/EP/T-amine/P-COOH adsorbents as temperature increase. Where the increase in q_L with temperature refers to a favorable adsorption of lanthanum ions at higher temperatures. The results (Table 2) show that Langmuir model fit experimental data well with higher R^2 values, indicating a suggested monolayer chemical adsorption of lanthanum ions on the PSWC/EP/T-amine and PSWC/EP/T-amine/P-COOH adsorbents. Additionally, the consistency of the maximum adsorption capacities of Langmuir model (Q_L) at different temperature with the corresponding experimental values (q_e) confirms the formation of monolayer adsorption system according to Langmuir model hypothesis. According to Eq. 8, the monolayer surface coverage (θ) is related to the values of lanthanum initial concentration and Langmuir binding constant [32].

$$\theta = \frac{K_L C_i}{1 + K_L C_i} \quad (8)$$

The values of θ were calculated using Eq. 11 (Table 2) and graphically depicted in Figure 8a (C_i versus θ). The results show a significant affinity of the used adsorbents towards lanthanum ions with high monolayer surface coverage ($\theta > 99\%$). The essential characteristics of Langmuir isotherm can be explained in terms of a dimensionless constant, separation factor, R_L , (Eq. 9). The value of R_L is used to determine the feasibility of the adsorption process, indicating the compatibility of the biosorption

processes (positive values ($0 < R_L < 1$)) refer to a feasible adsorption process otherwise not feasible (linear, $R_L = 1$, or irreversible, $R_L = 0$) [33].

$$R_L = \frac{1}{1 + K_L C_i} \quad (9)$$

Equation 9 was illustrated graphically in Figure 8b, and the obtained R_L values were tabulated (Table 2). The positive R_L values obtained for both adsorbents are between 0.05 and 0.62 (so, $0 < R_L < 1$), indicate that lanthanum adsorption is feasible on all developed adsorbents.

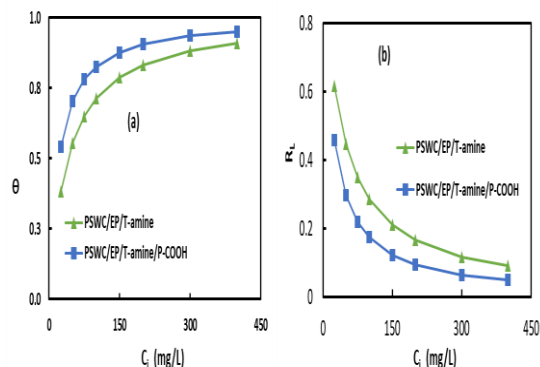


Fig. 8. The monolayer surface coverage (a) and separation factor (b) for lanthanum adsorption by PSWC/EP/T-amine and PSWC/EP/T-amine/P-COOH.

The Freundlich model (Eq. 10), was among the first models to be created to describe the adsorption processes, it is an empirical relationship applied to describe the non-ideal adsorption processes [34]. As a result, it is regarded as a model that incorporates the measure of heterogeneous adsorption. The adsorbent surface should be more heterogeneous if the equation's heterogeneity factor exceeds one.

$$\log q_e = \frac{1}{n} \log C_e + \log K_F \quad (10)$$

where K_F and $1/n$ are adsorption capacity and heterogeneity constant of Freundlich model. The values of $(\log q_e)$ of lanthanum adsorption by PSWC/EP/T-amine and PSWC/EP/T-amine/P-COOH adsorbents at different temperatures were modelled vs the corresponding values of $(\log C_e)$, Fig. S5, Supplementary file. The Freundlich model's linear regression give straight lines with slope and intercept equals the value of $(\log K_F)$ and $(1/n)$. The values of K_F and n were calculated and were tabulated (Table 2). The value of heterogeneity constant (n , 0.91 – 1.47) suggested a favorable lanthanum adsorption on PSWC/EP/T-amine and PSWC/EP/T-amine/P-COOH adsorbents at all studied temperatures. The small values of the correlation coefficient ($R^2 \leq 0.92$) indicate that Freundlich isotherm did not fit well the lanthanum adsorption on PSWC/EP/T-amine and PSWC/EP/T-amine/P-COOH adsorbents. Dubinin-Radushkevich isotherm is a temperature-dependent model may be used to predict mechanism of adsorption process.

Energy of adsorption process can be calculated from Dubinin-Radushkevich isotherm and subsequently the mechanism of adsorption process can be predicted. The equilibrium data of lanthanum adsorption by PSWC/EP/T-amine and PSWC/EP/T-amine/P-COOH adsorbents were modeled according to Dubinin-Radushkevich, Eq. 11 [32].

$$\ln q_e = \ln q_{DR} - K_{DR} \left(RT \ln \left[1 + \frac{1}{C_e} \right] \right)^2 \quad (11)$$

Where q_e (mmol/g), q_{DR} (mmol/g) and K_{DR} (mol²/kJ²) are the experimental adsorption capacity, theoretical adsorption capacity (according to Dubinin-Radushkevich model) and Dubinin-Radushkevich constant, respectively. R, T and C_e are the universal gas constant (8.314 J/mol K), absolute temperature (K) and equilibrium concentration of adsorbate (mmol/L), respectively. Another constant is the D-R isotherm constant (ε) was introduced in Eq. 11 where **Table 2**

The obtained isotherm and thermodynamics parameters of lanthanum adsorption on PSWC/EP/T-amine and PSWC/EP/T-amine/P-COOH adsorbents.

Adsorbent	Temp.		Langmuir parameters				Freundlich parameters		
	T K	Exp. q_e mg/g	q_L mg/g	K_L mg/g	R^2	n	K_n mg/g	R^2	
PSWC/EP/T-amine	298	75.8	86.21	0.0246	0.9946	2.41	8.18	0.8762	
	308	82.2	90.91	0.0287	0.9981	2.71	11.09	0.9019	
	318	89.4	98.04	0.0342	0.9982	2.94	36.31	0.9200	
	328	98.2	104.17	0.0489	0.9981	3.42	20.60	0.9012	
PSWC/EP/T-amine/P-COOH	298	101.8	112.32	0.0473	0.9987	3.10	19.22	0.8560	
	308	112.6	119.05	0.0500	0.9992	3.125	20.94	0.8465	
	318	121.8	128.21	0.0565	0.9995	3.39	25.66	0.8867	
	328	129.6	133.33	0.0610	0.9984	3.60	29.40	0.8902	
Adsorbent	Thermodynamics parameters				Dubinin-Radushkevich parameters				
	T K	ΔH° J/mol	ΔS° J/mol.K	ΔG° J/mol	q_{DR} mmol/g	E mg/g	R^2		
PSWC/EP/T-amine	298	18063	127.86	-20040	0.57	78.68	0.9945		
	308	18063	127.86	-21318	0.59	81.48	0.9877		
	318	18063	127.86	-22597	0.64	88.36	0.9803		
	328	18063	127.86	-23875	0.70	96.74	0.9725		
PSWC/EP/T-amine/P-COOH	298	7208	97.17	-21747	0.77	107.46	0.984		
	308	7208	97.17	-22719	0.83	115.43	0.9931		
	318	7208	97.17	-2369	0.85	118.51	0.9703		
	328	7208	97.17	-24662	0.88	122.19	0.9778		

The apparent energy (E) of lanthanum adsorption process can be calculated from the calculated values of K_{DR} and subsequently the type of the sorption process can be predicted. The values of E were calculated using Eq. 12 [32].

$$E = \left[\frac{1}{\sqrt{2K_{DR}}} \right] \quad (12)$$

The calculated apparent energy values of lanthanum adsorption on PSWC/EP/T-amine and PSWC/EP/T-amine/P-COOH adsorbents were calculated (Table 2). The values of E fall within the physisorption reaction range (3.54 – 5.00 kJ/mol) for of lanthanum adsorption on PSWC/EP/T-amine. Whereas for PSWC/EP/T-amine/P-COOH, E values fall within the chemisorption reaction range (4.08 – 7.07 kJ/mol) for of lanthanum adsorption on PSWC/EP/T-amine/P-COOH adsorbent.

its value equals the value of $(RT \ln[1+1/C_e])$. The values of $(\ln q_e)$ of lanthanum adsorption by PSWC/EP/T-amine and PSWC/EP/T-amine/P-COOH adsorbents at different temperatures were charted vs the corresponding values of (ε^2) . The Dubinin-Radushkevich model's linear regression give straight lines with slope and intercept equals the value of $(-K_{DR})$ and $(\ln q_{DR})$, respectively (Figure 9). The values of q_{DR} and K_{DR} were calculated from with slope and intercept of the straight lines (Table 2). The higher values of the R^2 (≥ 0.9703) indicate the suitability of Dubinin-Radushkevich isotherm to fit lanthanum adsorption on the adsorbents. Also, the value of the theoretical adsorption capacity of Dubinin-Radushkevich model are consistent with the experimental data.

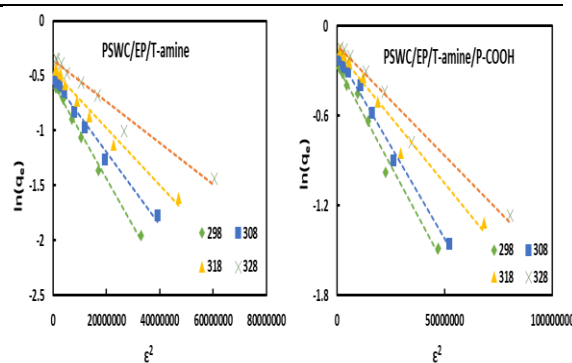


Fig. 9. The Dubinin-Radushkevich isotherm for lanthanum adsorption by PSWC/EP/T-amine and PSWC/EP/T-amine/P-COOH

3.8. Effect of the PSWC/EP/T-amine and PSWC/EP/T-amine/P-COOH Dose

Evaluating effect of the adsorbent dose on the adsorption processes is very important parameter in designing practical adsorption system. Fig. S6 (Supplementary file) shows the role of the adsorbent dose on lanthanum adsorption by PSWC/EP/T-amine and PSWC/EP/T-amine/P-COOH adsorbents. According to the findings, the uptake efficiency are increased as the PSWC/EP/T-amine and PSWC/EP/T-amine/P-COOH dose increased. This may be attributed to the significantly raise in the number of active sites of PSWC/EP/T-amine and PSWC/EP/T-amine/P-COOH (due to increase their concentrations), and hence increase lanthanum capture. The maximum lanthanum uptake efficiency of PSWC/EP/T-amine and PSWC/EP/T-amine/P-COOH adsorbents reached a value of 82.8 % and 91.2 %, respectively. These higher lanthanum uptake efficiency suggesting a promising applications of PSWC/EP/T-amine and PSWC/EP/T-amine/P-COOH adsorbents. The decrease in uptake capability with increasing PSWC/EP/T-amine and PSWC/EP/T-amine/P-COOH doses might be a consequence of decrease lanthanum ions/ adsorbent active site ratio.

3.9. Thermodynamic Studies

The adsorption thermodynamics study may be used to identify a number of thermodynamic characteristics. These thermodynamic characteristics reveal details about the sorption mechanism and nature. The most often researched thermodynamic characteristics are Gibbs free energy (ΔG° , minimal isothermal work required for the adsorbent to reach a given energy level.), enthalpy (ΔH° , heat adsorbed or released during the adsorption process), and entropy change (ΔS° , adsorption entropy offers information on the randomness and packing of the adsorbed species). The nature adsorption process may be endothermic (positive enthalpy change) or exothermic (negative enthalpy change). In the exothermic adsorption process, it is important to quantify the heat of adsorption to ensure the operation is safe. If the heat of adsorption is accumulated in the system, excess heating in the workplace or an explosion could bring hazards. Apart from that, the released heat will alter the sorbent temperature and subsequently affect the operation because there are changes in the mass transfer and adsorption process [45]. Also, the adsorption process may be classified as either chemical, physical, or physical/chemical process. The range of enthalpy change (ΔH°), or more precisely the heat of adsorption, distinguishes these forms of adsorption. A physical adsorption's heat is between 8 and 25

kJ/mol, whereas a chemical adsorption's heat is between 40 and 200 kJ/mol of energy. To assure the success of an adsorption process, it is crucial to measure the heat of adsorption. Van't Hoff equation (Eq. 13) was used to compute the thermodynamic characteristics (ΔG° , ΔH° , ΔS°) of lanthanum adsorption by PSWC/EP/T-amine and PSWC/EP/T-amine/P-COOH adsorbents were using [34]:

$$\ln K_L = -\frac{1}{RT}\Delta H^\circ + \frac{1}{R}\Delta S^\circ \quad (13)$$

The equilibrium data (values of Langmuir binding constant (K_L) obtained at different temperature and their corresponding adsorption medium temperature (T)) of lanthanum adsorption by PSWC/EP/T-amine and PSWC/EP/T-amine/P-COOH adsorbents were modeled according to van't Hoff equation. According to van't Hoff equation, plotting the values of ($\ln K_L$) against the values of ($1/T$) of lanthanum adsorption by PSWC/EP/T-amine and PSWC/EP/T-amine/P-COOH adsorbents gives straight line with slope and intercept equals the value of ($-\Delta H^\circ/R$) and ($\Delta S^\circ/R$), respectively. The van't Hoff's linear regression is shown in Fig. S7 (Supplementary file). The ΔH° and ΔS° values at different temperatures were calculated, and were given in Table 2. Clearly, the positive values of ΔH° (18.63 KJ/mol) refers to an endothermic physical adsorption of lanthanum adsorption on PSWC/EP/T-amine adsorbent. On the other side, the positive values of ΔH° (72.09 KJ/mol) refers to an endothermic chemical adsorption of lanthanum adsorption on PSWC/EP/T-amine/P-COOH adsorbent (mainly ion exchange mechanism). The positive values of ΔS° refers to increase randomness during adsorption of lanthanum adsorption by PSWC/EP/T-amine and PSWC/EP/T-amine/P-COOH adsorbents. The calculated ΔH° and ΔS° values may be used to compute the Gibbs free energy (ΔG° , minimal isothermal work required for the adsorbent to reach a given energy level) of the adsorption reaction of lanthanum with the studied adsorbents, Eq. 14 [34].

$$\Delta G^\circ = -T\Delta S^\circ + \Delta H^\circ \quad (14)$$

The calculated values of Gibbs free energy are given in Table 2 Obviously, all the obtained Gibbs free energy values are negative values (from -20.04 to -24.66 kJ/mole) confirming the spontaneous nature of lanthanum adsorption on PSWC/EP/T-amine and PSWC/EP/T-amine/P-COOH adsorbents. Also, increasing the Gibbs free energy negative values suggests that lanthanum adsorption becomes more favorable with increasing of temperature.

3.10. Elution and Regeneration of the PSWC/EP/T-amine and PSWC/EP/T-amine/P-COOH Loaded Biosorbents

The elution of the adsorbed lanthanum ions from the PSWC/EP/T-amine and PSWC/EP/T-amine/P-COOH loaded biosorbents was investigated using 0.5 N HCl solution. 25 mg of the lanthanum-loaded biosorbents was agitated in 50 mL of the acid solution overnight. The PSWC/EP/T-amine and PSWC/EP/T-amine/P-COOH were filtered and the elution mediums were analyzed to determine lanthanum elution percentage. Five sequential adsorption/elution cycles were used to assess the reusability of the biosorbent. After elution experiment, the PSWC/EP/T-amine and PSWC/EP/T-amine/P-COOH adsorbents was rinsed in water (to pH = 7) before to the next adsorption cycle. The results of adsorption/elution cycle show promising elution percent of about 96.5 and 95.2 % from La (III) lanthanum-PSWC/EP/T-amine and lanthanum-PSWC/EP/T-amine/P-COOH adsorbents, respectively. The biosorbent regeneration percent after five cycle PSWC/EP/T-amine and PSWC/EP/T-amine/P-COOH adsorbents is about 84%. In addition, the adsorption capacity of the five cycle capacity equals 86.4 - 88.4% of corresponding value of the first cycle.

3.11. Case Study

The Egyptian black sands occupy about 700 km along the Mediterranean Sea coastal zone from the Abu-Qir area in the west to the Rafah area in the east, and they are found either as beach deposits or accumulated sand dunes along the shore-line (Fig. 10). The Egyptian black sands encounter several important minerals in economic reserves, such as magnetite, ilmenite, zircon, monazite, garnet, cassiterite, and rutile, in addition to the native gold. These sands are believed to be sourced from different basement rocks (igneous and metamorphic) found in the upper reaches of the Nile River, the Ethiopian Plateau, and heights of East Central Africa; in particular, the monazite mineral was suggested as a probable derivative of granite and pegmatite rocks of the White Nile provenance [35].

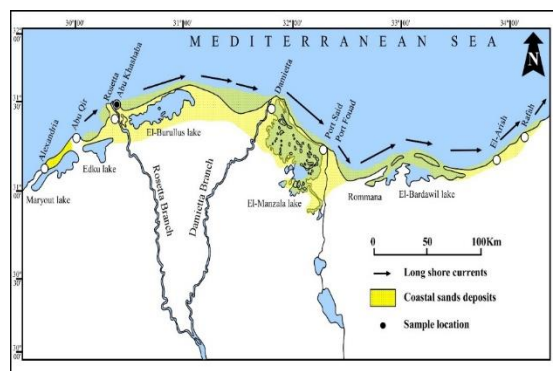


Fig. 10. A map exhibits the black sand distribution along the Egyptian North Coast and shows the location of the Abu-Khashaba area.

From the geological reserve point of view, the Egyptian black sands were estimated at 647 million metric tons in total, and this amount was divided into about 31 million metric tons in the upper top zone of the beach and about 616 million metric tons in the following twenty meters. The monazite component was estimated to form about 0.01–0.6% of the total black sands volume; this variation is mainly related to the concentration of the present black sands and to the natural concentration process (the eroded beach zones have a higher monazite concentration than the un-eroded areas). Although the relative importance of each mineral constituent in black sand varies, the monazite mineral garners special attention due to its chemical composition, which is rich in REE and the elements thorium and uranium. Monazite is regarded as the main conventional source for REEs extraction and production, and non-conventional source for both thorium and uranium.

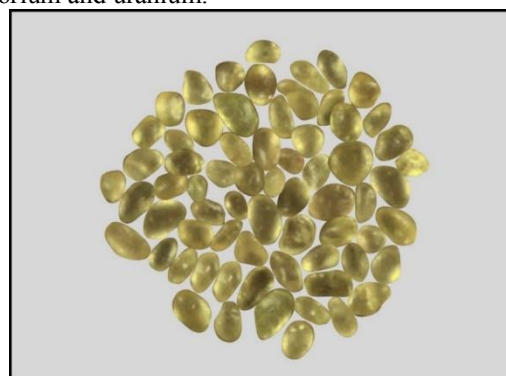


Fig. 11. High-grade monazite concentrate resulted from the concentration processes of the black sands.

3.11.1. Monazite Sample Preparation

To conduct a considerable amount of monazite mineral concentrate, ten black sand samples were

collected from the beach zone in the Abu Khashaba area, which extends 5 km in length and 0.5 km in width to the east of Rosetta distributaries on the Mediterranean coast. For utilization in the separation processes, the samples were collected vertically from the beach surface to about 35 cm depth and distributed horizontally along a 3 km distance (one sample/300 meters) to conduct representative samples of black sands containing monazite average concentration of about 0.1% as previously recorded in the bulk black sand in this region, then all the samples were carefully mixed into one technological black sands sample. Generally, the monazite concentrate is extracted from the black sand through a series of separation procedures i.e. (1) magnetic separation to separate ilmenite, magnetite, leucosene and other paramagnetic minerals from the technological black sands sample. This separated portion make up the great bulk of the technological black sands sample. (2) Electrostatic separation, after paramagnetic minerals, the residue of the sample (mainly composed of monazite and zircon minerals) was subject to electrostatic separation. The electrostatic separation yielding two fractions, conductor and non-conductor portions. The last fraction was fractionated using wet-table separation method. Two fraction was obtained from the last separation method (tail-table strip (mainly composed of zircon mineral) and top-table strip (mainly composed of monazite mineral). Monazite concentration with high grad ($\geq 92\%$) was found to be the dominant constituent in the top-table strip portion. Fig. 11 shows the microscopic image of the obtained monazite sample results from the concentration processes of the black sands. The size of the obtained monazite concentrate sample was reduced to a representative portion of 50 grams by the quartering technique (by which the sample is split into two portions and then each portion is successively quartered to about 50 grams), ground to -200 mesh size, then mixed well, transferred, and stored in labeled plastic vials. This finely ground portion is suitable for chemical analysis. Table 3 shows the chemical composition of the monazite solid sample.

Table 3
Chemical composition of the monazite sample

Components	Concentration		
	Wt., %	RE ₂ O ₃ Concentration	
RE ₂ O ₃	54.67	La ₂ O ₃	12.24
P ₂ O ₅	28.11	CeO ₂	23.27
ThO ₂	6.53	Pr ₂ O ₃	2.76
Fe ₂ O ₃	2.74	Nd ₂ O ₃	9.99
TiO ₂	2.62	Sm ₂ O ₃	2.04
CaO	0.98	Gd ₂ O ₃	1.30
SiO ₂	1.2	Dy ₂ O ₃	0.88
U ₃ O ₈	0.41	Ho ₂ O ₃	0.25
Total	97.26	Y ₂ O ₃	1.76

3.11.2. Monazite Chemical Leaching

The obtained monazite powder was digested using sulfuric acid route. In details, the monazite concentrate was fed through portions to sulfuric acid at 463 K. The other leaching conditions are solid/liquid ratio of 1/4, leaching temperature of 498 K (after complete addition of the obtained monazite powder to sulfuric acid at 463 K, the reaction temperature was raised to 498 K) and leaching time of 4h. After 4h, nearly all REE content into the monazite sample residue was leached by cold water. The resultant leached monazite filtrate was analyzed to determine its REE concentration and other constituent content (Table 4).

3.11.3. Extract Lanthanum Ions from Monazite Leach Liquid

Lanthanum recovery was achieved by adding 0.5 g of PSWC/EP/T-amine and PSWC/EP/T-amine/P-COOH into 50 mL of the resultant leached monazite filtrate obtained from the previous. The PSWC/EP/T-amine and PSWC/EP/T-amine/P-COOH were removed from the monazite filtrate after 30 minutes of stirring, where residual content of lanthanum into the monazite filtrate was then measured to evaluate adsorption efficiency. The concentrations of REE on the leach liquor before and after treatment with PSWC/EP/T-amine and PSWC/EP/T-amine/P-COOH adsorbents were quantified using ICP-OES (Table 4). The adsorbents showed a higher affinities to extract lanthanum(III) from leach liquid. The lanthanum concentrations on the leach liquor decreased from 154.9 mg/L to 49.6 mg/L after first treatment with the PSWC/EP/T-amine adsorbent. On the other side, the PSWC/EP/T-amine/P-COOH adsorbent was more efficient than PSWC/EP/T-amine adsorbent in the lanthanum recovery. The lanthanum concentrations on the leach liquor decreased from 154.9 mg/L to 44.8 mg/L after first treatment with the PSWC/EP/T-amine/P-COOH adsorbent.

Table 4
The chemical composition of the monazite leach liquid

Metal ion	The concentration of metal ions in the leach liquor (mg/L)		
	Before treatment, C _i mg/l	PSWC/EP/T-amine	After treatment, C _e PSWC/EP/T-amine/P-COOH
La	154.92	49.6	44.8
Ce	294.56	95.4	89.1
Pr	34.9	12.9	11.8
Nd	126.56	45.3	38.7
Sm	25.76	12.3	11.2
Eu	0.04	0.03	0.02
Gd	16.48	11.4	10.2
Tb	1.22	1.6	1.4
Dy	11.12	10.7	9.3
Ho	3.16	2.9	2.6
Er	0.024	0.02	0.02
Tm	0.04	0.03	0.03
Yb	0.034	0.03	0.03
Lu	1.12	1.1	1
Y	22.24	19.9	17.8

4. Conclusions

PSWC/EP/T-amine and PSWC/EP/T-amine/P-COOH adsorbents were synthesized from shrimp waste using green synthesis approach, and were applied for lanthanum adsorption from synthetic and real samples. The uptake of lanthanum(III) ions by PSWC/EP, PSWC/EP/T-amine and PSWC/EP/T-amine/P-COOH was very low at pH < 1, and is increased with the increase of pH till reached maximum value at the limit of pH 7.0, for both adsorbents. The maximum uptake of lanthanum ions by PSWC/EP, PSWC/EP/T-amine and PSWC/EP/T-amine/P-COOH achieved at pH 7.0 were 57.4, 73.8 and 101.4 mg/g, respectively. The adsorption capacity of lanthanum ions on PSWC/EP/T-amine and PSWC/EP/T-amine/P-COOH rose monotonically till it arrive the plateau at 150 minutes. About 25.88 and 29.23% of the total adsorbed lanthanum ions were adsorbed in less than 10 minutes by PSWC/EP/T-amine and PSWC/EP/T-amine/P-COOH, respectively.

5. Conflicts of interest

There are no conflicts to declare.

6. References

- [1] Chakhmouradian A.R. and Wall F., Rare earth elements: minerals, mines, magnets (and More). *Elements*, 8, 333-340 (2012). <https://doi.org/10.2113/gselements.8.5.333>.
- [2] Gschneider A.K. and Eyring L., Handbook of the physics and chemistry of rare earths, Vol I, North-Holland, Amsterdam (1978).
- [3] Abhilash S. ., Meshram P., Pandey B.D., Metallurgical processes for the recovery and recycling of lanthanum from various resources-A review. *Hydrometallurgy*, 160, 47-59 (2016). <https://doi.org/10.1016/j.hydromet.2015.12..4>
- [4] Cotton S., Lanthanides and Actinides. Oxford University Press (1991).
- [5] Greenwood N.N. and Earnshaw A., Chemistry of the elements. Second edition, Elsevier, 1227-1249 (2006).
- [6] Johnson D.A., Principles of Lanthanide Chemistry. *J.Chem. Ed.* 57, 475-477 (1980).
- [7] De lima I.B. and Filho W.L., Rare earths industry: technological, economic, and environmental implications. Elsevier, USA (2016).
- [8] Díaz-Flores P.E., Arcibar-Orozco J.A., Flores-Rojas A.I., Rangel-Méndez J.R., Synthesis of a chitosan-zeolite composite modified with La(III): characterization and its application in the removal of fluoride from aqueous systems. *Water Air Soil Pollut.*, 232, 235 (2021). <https://doi.org/10.1007/s11270-021-05185-1>
- [9] Zhang Y., Zheng X., Bian T., Zhang Y., Mei J., Li Z., Phosphorylated-CNC/MWCNT thin films-toward efficient adsorption of rare earth La(III). *Cellulose* 27, 3379-3390 (2020). <https://doi.org/10.1007/s10570-020-03012-0>
- [10] Jiménez-Reyes M., Ramírez De La Cruz F.deM., Solache-Ríos M., Physicochemical behavior of uranium and lanthanum in the presence of *Abies religiosa* Leaf biomass. *Water Air Soil Pollut.* 231, 469 (2020). <https://doi.org/10.1007/s11270-020-04822-5>
- [11] da Costa B., da Silva M.G.C., Vieira M.G.A. Biosorption of rare-earth and toxic metals from aqueous medium using different alternative biosorbents: evaluation of metallic affinity.

- Environ Sci Pollut Res 29, 79788–79797 (2022). <https://doi.org/10.1007/s11356-021-16506-6>
- [12] Peter S., Lyczko N., Gopakumar D., Maria H.J., Nzihou A., Thomas S., Chitin and chitosan based composites for energy and environmental applications: a review. *Waste Biomass Valor*, 12, 4777-4804 (2021). <https://doi.org/10.1007/s12649-020-01244-6>.
- [13] Guo N., Sun J., Zhang Z., Moa X., Recovery of chitin and protein from shrimp head waste by endogenous enzyme autolysis and fermentation. *J. Ocean Univ. China*, 18, 719–726 (2019). <https://doi.org/10.1007/s11802-019-3867-9>.
- [14] Lahiji M.N., Keshkar A.R., Moosavian M.A., Adsorption of cerium and lanthanum from aqueous solutions by chitosan/polyvinyl alcohol/3-mercaptopropyltrimethoxysilane beads in batch and fixed-bed systems. *Particulate Science and Technology*, 36, 340-350 (2018). <https://doi.org/10.1080/02726351.2016.1248262>
- [15] Zhao F., Yang Z., Wei Z., Spinney R., Sillanpää M., Tang J., Tam M., Xiao R., Polyethylenimine-modified chitosan materials for the recovery of La(III) from leachates of bauxite residue. *Chemical Engineering Journal*, 388, 124307 (2020). <https://doi.org/10.1016/j.cej.2020.124307>
- [16] Ramasamy D.L., Wojtuś A., Repo E., Kalliola S., Srivastava V., Sillanpää M., Ligand immobilized novel hybrid adsorbents for rare earth elements (REE) removal from waste water: Assessing the feasibility of using APTES functionalized silica in the hybridization process with chitosan. *Chemical Engineering Journal*, 330, 1370-1379 (2017). <https://doi.org/10.1016/j.cej.2017.08.098>
- [17] Khalil M.M.H., Atrees M.S., Abd El Fatah A.I.L., Salem H., Roshdi R., Synthesis and application studies of chitosan acryloylthiourea derivative for the separation of rare earth elements. *Journal of Dispersion Science and Technology*, 39, 605-613 (2018). <https://doi.org/10.1080/01932691.2017.1370674>
- [18] Mahmoud M.E., Ibrahim G.A.A., Abdelwahab M.S., Manganese dioxide nanoparticles decorated with chitosan for effective removal of lead and lanthanum ions from water by microwave sorption technique. *Materials Science and Engineering B*, 267, 115091 (2021). <https://doi.org/10.1016/j.mseb.2021.115091>
- [19] Marczenko Z., Separation and spectrophotometric determination of elements, Ellis Harwood, Chichester (1986).
- [20] Ibrahim M.M., El-Sheshtawy H.S., Abd El-Magied M.O., Manaa E.S.A., Youssef M.A.M., Kouraim M.N., Eldesouky E.M., Dhmees A.S., A facile and cost-effective adsorbent derived from industrial iron-making slag for uranium removal. *J Radioanal Nucl Chem*, 329, 1291-1300 (2021). <https://doi.org/10.1007/s10967-021-07914-6>.
- [21] Nandiyanto A.B.D., Oktiani R., Ragadhita R., How to read and interpret FTIR spectroscopy of organic material. *Indonesian Journal of Science & Technology*, 4, 97-118 (2019). <https://doi.org/10.17509/ijost.v4i1.15806>.
- [22] Movasaghi Z., Rehman S., Rehman Dr.I.u., Fourier transform infrared (FTIR) spectroscopy of biological tissues. *Applied Spectroscopy Reviews*, 43, 134-179 (2008). <http://dx.doi.org/10.1080/05704920701829043>.
- [23] Abd El-Magied M.O., Manaa E.A., Korim M.N., Mahmoud M.A., Eldesouky E.M., Solid-liquid phase extraction of thorium (IV) from nitrate leach liquors using amine functionalized glycidyl methacrylate resins. *Nuclear Sciences Scientific Journal*, 9, 187-196 (2020). <https://doi.org/10.21608/nssj.2020.265514>.
- [24] Alharthi S., Alharthy S.A., Manaa E.-S.A., Abd El-Magied M. O., Salem W. M., High adsorption performance of Cr(VI) ions from the electroplating waste solution using surface-modified porous poly 2-((methacryloxy)methyl)oxirane polymers. *Z. Anorg. Allg. Chem.*, 648, e202100327 (2022). <https://doi.org/10.1002/zaac.202100327>.
- [25] Costa T., Silva M., Vieira M., Evaluation of metal affinity of lanthanum using different alternative bio/adsorbent materials. *Chemical Engineering Transactions*, 74, 1129-1134 (2019). <https://doi.org/10.3303/CET1974189>.
- [26] Negm S.H., Abd El-Magied M.O., El Maadawy W.M., Abdel Aal M.M., Abd El Dayem S.M., Taher M.A., Abd El-Rahem K.A., Rashed M.N., Cheira M.F., Appreciatively efficient sorption achievement to U(VI) from the El Sela area by ZrO₂/Chitosan. *Separations*, 9, 311 (2022). <https://doi.org/10.3390/separations9100311>.
- [27] Abd El-Magied M.O., Abd El Fatah A. I. L., Mashaal H., Tawfique A., Alhindawy I. G., Manaa E.-S. A., Elshehy E. A. Fabrication of worm-like mesoporous silica monoliths as an efficient sorbent for thorium ions from nitrate media. *Radiochemistry*, 64, 62–73 (2022). <https://doi.org/10.1134/S1066362222010106>.
- [28] Abd El-Magied M.O., Dhmees A.S., Abd El-Hamid A.A.M., Eldesouky E.M., Uranium extraction by sulfonated mesoporous silica derived from blast furnace slag. *Journal of Nuclear Materials*, 509, 295-304 (2018). <https://doi.org/10.1016/j.jnucmat.2018.06.034>.
- [29] Ho Y.S., Review of second-order models for adsorption systems. *Journal of Hazardous Materials*, 136, 681-689 (2006). <https://doi.org/10.1016/j.jhazmat.2005.12.043>.
- [30] Lau L.C., MohamadNor N., Lee K.T., Mohamed A.R., Adsorption isotherm, kinetic,

- thermodynamic and breakthrough curve models of H₂S removal using CeO₂/NaOH/PSAC. *Int J Petrochem Sci Eng.*, 1, 36-44 (2016). <https://doi.org/10.15406/ipcse.2016.01.00009>.
- [31] Sadeek S.A., El-Sayed M.A., Amine M.M., Abd El-Magied M.O., A chelating resin containing trihydroxybenzoic acid as the functional group; synthesis and adsorption behavior for Th(IV) and U(VI) ions. *J. Radioanal. Nucl. Chem.*, 299, 1299-1306 (2014). <https://doi.org/10.1007/s10967-013-2847-6>.
- [32] Abu El-Soad A.M., Abd El-Magied M.O., Atrees M.S., Kovaleva E.G., Lazzara G., Synthesis and characterization of modified sulfonated chitosan for beryllium recovery. *Int. J. Biol. Macromol.*, 139, 153-160 (2019). <https://doi.org/10.1016/j.ijbiomac.2019.07.162>.
- [33] Tag El-Din A.F., Elshehy E.A., Abd El-Magied M.O., Atia A.A., El-Khouly M.E., Decontamination of radioactive cesium ions using ordered mesoporous monetite. *RSC Adv.*, 8, 19041-19050 (2018). <https://doi.org/10.1039/C8RA02707B>.
- [34] Sadeek S.A., Moussa E.M.M., El-Sayed M.A., Amine M.M., Abd El-Magied M. O., Uranium(VI) and thorium(IV) adsorption studies on chelating resin containing pentaethylenhexamine as a functional group. *J. Dispers. Sci. Technol.*, 35, 926-933 (2014). <https://doi.org/10.1080/01932691.2013.809507>.
- [35] El-Kammar A.A., Ragab A.A., Moustafa M.I., Geochemistry of economic heavy minerals from Rosetta black sand of Egypt. *Journal of King Abdulaziz University: Earth Sciences*, 22, 69-97 (2011). <https://doi.org/10.4197/ear.22-2.4>.